Theory of Jahn–Teller distortions of the P donor in diamond

2005 J. Phys.: Condens. Matter 17 5831

(http://iopscience.iop.org/0953-8984/17/37/018)

INSTITUTE OF PHYSICS PUBLISHING JOURNAL OF PHYSICS: CONDENSED MATTER

J. Phys.: Condens. Matter **17** (2005) 5831–5837 doi:10.1088/0953-8984/17/37/018

Theory of Jahn–Teller distortions of the P donor in diamond

R J Eyre, J P Goss, P R Briddon and J P Hagon

School of Natural Sciences, University of Newcastle upon Tyne, Newcastle upon Tyne, NE1 7RU, UK

E-mail: J.P.Goss@ncl.ac.uk

Received 11 July 2005, in final form 14 August 2005
Published 2 September 2005
Online at stacks.iop.org/JPhysCM/17/5831

Abstract

Phosphorus, the current standard n-type dopant in diamond, has been correlated with isotropic, trigonal and tetragonal paramagnetic centres, suggesting that it may undergo a symmetry lowering distortion, perhaps of a Jahn–Teller type. We present first-principles calculations for examining the energetics of various sub-group symmetries of the on-site, tetrahedral donor, and show that C_{2v}, C_{3v} and D_{2d} conformations reduce the total energy and conform to the Jahn–Teller theorem. We also present a qualitative explanation of the resulting quantum-mechanical states. The small amount of energy saved by the distortion may indicate a dynamic Jahn–Teller effect.

1. Introduction

The application of diamond to electronics has, in common with other wide-gap materials, significant obstacles due to difficulty in achieving high levels of shallow dopants. Diamond of p-type is readily obtained using boron acceptors, but the natural n-type dopant, nitrogen, has a deep donor level at $E_c - 1.7$ eV [1]. Despite theoretically being insoluble [2–4], doping with substitutional P (P_s) has proved the most reliable and best understood method of n-type doping of diamond, but with a rather deep donor level ($\sim E_c - 0.6$ eV [5–7]). Nevertheless, concentrations of P of 10^{19} cm^{-3} have been achieved [8], and devices demonstrated [9–12].

Electron paramagnetic resonance (EPR) experiments that determine the symmetry of systems with unpaired electrons have detected P-related centres via hyperfine interactions with the ^{31}P nuclei [13–17]. In implanted and annealed material, an isotropic EPR centre was detected at 20 K that correlates with infrared (IR) electronic transitions at 4220 and 4535 cm^{-1} associated with the P donor [15]. Another centre detected electrically may also be related to P [16]. This system has C_{3v} symmetry at 120 K. However, the signal has only around 2% spin density on P, and may be due to a P–X complex. Finally, the most recent EPR experiments detected a tetragonal [17] centre at 30 K with an estimated concentration around 5% of the

Table 1. Orbital symmetries correlated with the on-site t_2 one-electron levels produced by lowering the symmetry of P_s to C_{2v}, C_{3v} and D_{2d}. The ordering of the split components is not dictated by symmetry. The possible many-electron symmetries associated with each point group are also listed. Only orbitally non-degenerate representations (A and B) satisfy the Jahn–Teller theorem.

Point group	T_d	C_{2v}	C_{3v}	D_{2d}
One-electron levels	t_2	$a_1 + b_1 + b_2$	$a_1 + e$	$b_2 + e$
Many-electron states	$^2T_2$	$^2A_1, ^2B_1, ^2B_2$	$^2A_1, ^2E$	$^2B_2, ^2E$

estimated concentration of P films grown homo-epitaxially on (111) oriented substrates. Again, this centre may be related to P donors.

Theoretically, we and others previously found a distortion of the neutral donor to C_{3v} symmetry [3, 18, 19]. Other theory has found P_s to stay on site [20, 21] or distort [22, 23]. We note that, although earlier theoretical studies reported a non-degenerate donor state for on-site P_s [20], most recent calculations suggest that the unpaired electron of an on-site P donor lies in a triply degenerate, t_2 level [3]. A distortion from T_d symmetry can then be understood within the Jahn–Teller theorem, which states that the centre will distort to a lower point-group symmetry such that the final system has an orbitally non-degenerate many-electron wavefunction.

Potential distortions within the Jahn–Teller framework will split the t_2 levels, with the nature of the splitting dependent on the magnitude and direction of the distortion. Although any sub-group of T_d is a candidate, of particular interest are those indicated by experiment, namely trigonal and tetragonal. The way that the t_2 levels split in the C_{2v}, C_{3v} and D_{2d} point groups and the potential many-electron states that ensue are listed in table 1.

Stimulated by the apparent contradictory experimental and theoretical evidence, we have used local-spin-density-functional methods to analyse potential Jahn–Teller distortions for P in diamond. In the following section we outline the method we employ, and present the results in section 3.

2. Method

Local-spin-density-functional calculations were carried out using `AIMPRO` (Ab Initio Modelling Program) [24] with periodic boundary conditions using 64-, 216- and 512-atom cubic supercells ($na_0 \times na_0 \times na_0$, $n = 2, 3, 4$).

The wavefunction basis consists of Gaussian functions centred at each atom. For carbon, the basis functions are combinations of eight s and p Gaussian functions, with the addition of five d Gaussian polarization functions. For P the basis consists of independent s, p and d Gaussians with five widths. The charge density is Fourier transformed using plane-waves with a cut-off of 650 Ryd. The lattice constant and bulk modulus of diamond are within $\sim$1 and 5% respectively of the experimental values, while the direct and indirect bandgaps, at 5.68 eV and 4.26 eV, respectively, are close to previously published plane-wave LDA values [25].

The band-structure was sampled either at the Γ point or a regular mesh of $2 \times 2 \times 2$ **k** points according to the Monkhorst–Pack scheme ($MP2^3$) [26]. Sampling the Brillouin zone may have significant implications for the treatment of Jahn–Teller systems. Given the potentially small distortions, it is important to have a sufficiently converged sampling scheme to correctly model the charge-density and electronic properties of the system. However, sampling away from the zone-centre generally raises orbital degeneracies, i.e. the degeneracies of gap-states will be dictated not only by the symmetry group of the defect geometry, but also by the little groups of the special k points. For example, an $MP2^3$ scheme folded according to the T_d point group results in a single point at $(0.25, 0.25, 0.25)2\pi/a_0$, at which all electronic functions

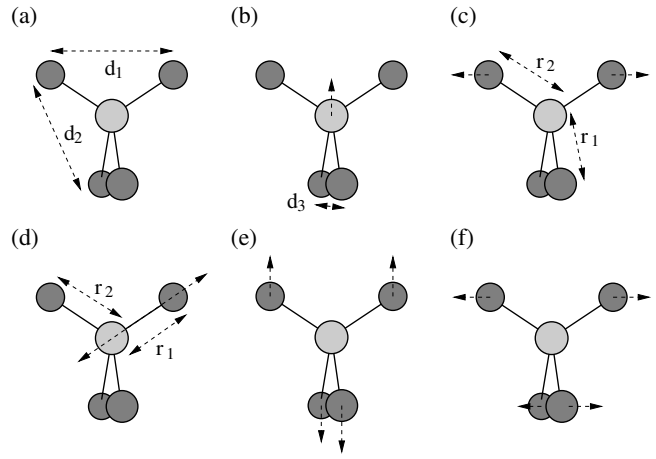

Figure 1. Schematic diagram showing the distortions to high-symmetry configurations of P_s and its nearest neighbours in diamond. (a) On-site, (b) and (c) C_{2v}, (d) C_{3v} and (e) and (f) D_{2d}. For (b)–(f) the arrows indicate the sense of displacement to produce the desired point-group symmetry. In each case vertical is [001].

transform according to the C_{3v} point group. Examination of table 1 tells us that this could result in the t_2 levels being split into a_1 below e even without any structural distortion. One potential solution to this problem is to use the Γ-point approximation so that all states retain their full degeneracies, but this results, especially for smaller supercells, in a relatively poorer calculation [27]. This is mitigated somewhat by using larger and larger supercells, but the Γ point converges very slowly with system size, even for a relatively simple system of a neutral 1000-atom cubic supercell of bulk diamond ($5a_0 \times 5a_0 \times 5a_0$): we find the total energies differ by 0.2 eV for the Γ point and MP2[3].

3. Results

P_s was relaxed in cubic supercells, constrained to T_d, C_{3v}, C_{2v} or D_{2d} symmetry, with the atoms displaced as shown schematically in figure 1. Distortions to a given point group are not unique: in the D_{2d} case we examined two types of structure, as presented in figures 1(d) and (e), which we label $D_{2d}(1)$ and $D_{2d}(2)$, respectively. Stable and meta-stable structures with different symmetries were obtained in all cell sizes. The key structural data and relative energies are listed in table 2, with the orthorhombic structure being derived from an initial displacement shown in figure 1(b). The consistency between the results from the 216-atom and 512-atom supercell structures and energies give us some confidence in these results.

We explored the dependence of the final structure on the magnitude and sense of the initial displacements. For example, displacing the P atom along [001] (figure 1(b)) results in the meta-stable orthorhombic structure detailed in table 2, whereas displacing two neighbouring carbon atoms (figure 1(c)) results in relaxation to the higher symmetry $D_{2d}(2)$ structure. The sensitivity to initial structure and relatively small energies involved render it difficult to be conclusive as to the ground state structure, but this is consistent with the relatively small differences in final structure (e.g. bond-lengths).

Additionally, in order to assess the role of the Γ-point approximation, we ran the 216-atom supercell structures with MP2[3] sampling. The structures deviated only very slightly from those in table 2. The C_{2v}, C_{3v} and $D_{2d}(2)$ structures were found to be 1, 41 and 45 meV

Table 2. Structural (Å) and energetic (meV) data for P_s in diamond using Γ-point sampling for three supercell sizes. Nearest (r_1, r_2) and next-neighbour distances (d_1, d_2 and d_3) are defined for the different symmetries in figure 1. Theoretical bulk nearest- and next-nearest-neighbour distances are 1.53 and 2.50 Å, respectively. ΔE^t and Δt_2 are the reduction in total energy and the splittings of the t_2 levels relative to the lowest-energy component, respectively.

	r_1	r_2	d_1	d_2	d_3	ΔE^t	Δt_2	
$2a_0 \times 2a_0 \times 2a_0$: 64 atoms								
T_d	1.68		2.74			0	0	0
C_{2v}	1.70	1.66	2.74	2.75	2.72	58	140	202
C_{3v}	1.72	1.67	2.73	2.75		75	230	230
$D_{2d}(1)$	1.68		2.73	2.75		8	0	51
$D_{2d}(2)$	1.68		2.77	2.73		35	116	116
$3a_0 \times 3a_0 \times 3a_0$: 216 atoms								
T_d	1.68		2.75			0	0	0
C_{2v}	1.70	1.67	2.75	2.76	2.74	26	70	90
C_{3v}	1.68	1.71	2.75	2.76		30	95	95
$D_{2d}(1)$	1.68		2.74	2.76		5	0	29
$D_{2d}(2)$	1.69		2.77	2.74		20	66	66
$4a_0 \times 4a_0 \times 4a_0$: 512 atoms								
T_d	1.69		2.75			0	0	0
C_{2v}	1.70	1.67	2.75	2.76	2.74	20	57	64
C_{3v}	1.71	1.68	2.75	2.76		22	69	69
$D_{2d}(1)$	1.69		2.74	2.76		4	0	25
$D_{2d}(2)$	1.69		2.77	2.74		20	60	60

lower in energy than T_d, respectively, whereas the $D_{2d}(1)$ was 26 meV *higher* in energy. The difference between the sampling schemes indicates that the relative energies are not converged, but qualitatively supports the view that there is more than one type of distortion of P_s that can reduce the total energy.

In order to gain some understanding of the physical nature of the distortion it is useful to examine the electron orbitals. The on-site centre t_2 levels can be described as linear combinations of the sp^3 hybrids pointing along anti-bonding directions from the P atom, with a smaller additional contribution from sp hybrids on the four neighbouring C atoms. Figure 2 shows the charge density derived from these levels. The nature of the states subsequent to the distortions can be viewed as energetically favourable interactions between these eight sp lobes.

Indeed, the occupied level for the $D_{2d}(2)$ system in the 216-atom supercell, shown in figure 3(a), can be described as a bonding combination of two sets of four sp orbitals, introducing a π-bonding character. This is similar in nature to the distortion at the self-interstitial in diamond from D_{2d} to D_2 so that the p orbitals overlap [28]. The higher, unoccupied orbitals (not shown) are anti-bonding combinations of the sp hybrids, comprising an e doublet.

This contrasts with the $D_{2d}(1)$ highest occupied orbitals, which are an e doublet of π-bonding combinations oriented along x and y. The resultant ^2E many-body wavefunction symmetry remains subject to a further Jahn–Teller distortion. Indeed, displacing the P atom along the principal axis by just 10^{-4} Å to reduce the symmetry to C_{2v}, and relaxing, produced a structure indistinguishable from the orthorhombic structure detailed in table 2. Such a displacement for the $D_{2d}(2)$ structure recovers the $D_{2d}(2)$ geometry.

The C_{3v} form, which is marginally lowest in energy in the Γ-point calculations, results in an occupied a_1 level (see table 1) dominated by a single sp lobe, shown in figure 3(b).

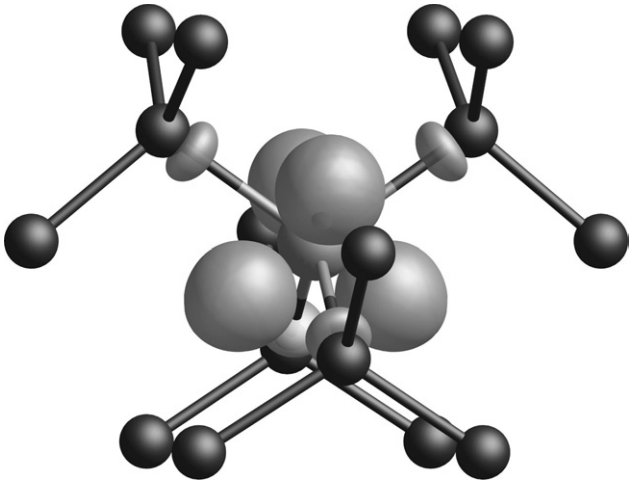

Figure 2. Schematic diagram indicating the nature of the t_2 levels at the Brillouin-zone centre for on-site, neutral P_s in diamond.

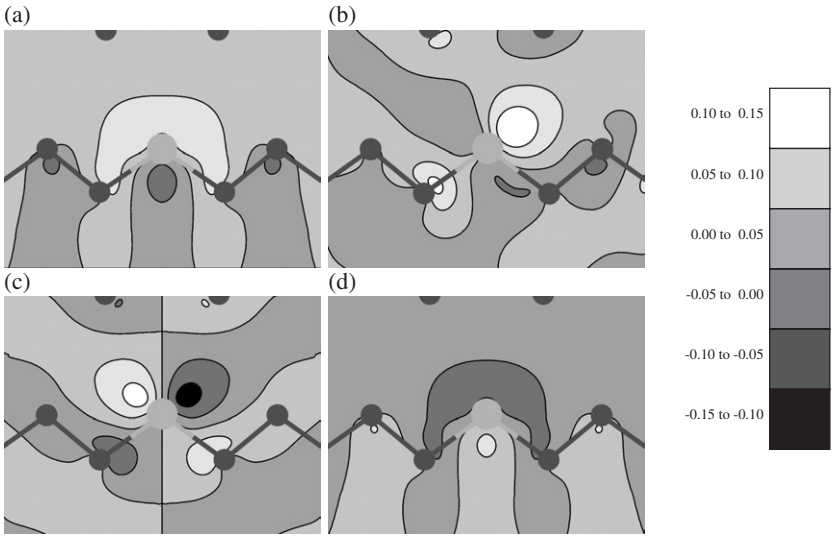

Figure 3. Contour plots of highest occupied, t_2-derived orbitals for (a) $D_{2d}(2)$, (b) C_{3v} and (c) C_{2v}. (d) The lowest unoccupied level for the C_{2v} structure to be compared with the occupied level of $D_{2d}(2)$, (a). Contours correspond to lines of constant wavefunction amplitude as indicated by the legend. The central atom is P, and the axes are [110] and [001] for horizontal and vertical, respectively.

Finally, the C_{2v} system reduces the t_2 levels to b_1, a_1 and b_2 levels in ascending order of energy. The three levels are easily understood in terms of the sp lobes of the undistorted system. Indeed, they also relate closely to those of the $D_{2d}(2)$ system with the b_1 and b_2 levels of the orthorhombic system closely resembling the two components of the $D_{2d}(2)$ e levels, being comprised of anti-bonding combinations (figure 3(c)). Additionally, the C_{2v} level with a_1 symmetry closely resembles that of $D_{2d}(2)$ b_1, being made up from π-bonding pairs, shown in figure 3(d).

In order to assess the periodic boundary condition, we also examined P_s in large atomic clusters. These calculations also yielded stable C_{3v} and $D_{2d}(2)$ structures.

4. Summary

We have analysed the nature of the phosphorus donor in diamond. The on-site defect has a one-electron configuration t_2^1, rendering it a Jahn–Teller system. The donor wavefunctions are related to sp hybrids pointing toward interstitial spaces in the diamond lattice.

In large supercells we find that there are a number of distortions generating at least metastable C_{2v}, C_{3v} and D_{2d} symmetry, corresponding to $^2B_1$, $^2A_1$ and $^2B_2$ orbitally non-degenerate many-body symmetries, respectively. Of these, trigonal and tetragonal symmetry are also stable in large atomic clusters. The stabilization of the tetragonal distortion may be thought of as arising from a weak π-bonding interaction between pairs of P-related sp lobes, also involving sp hybrids on the neighbouring C atoms.

In the context of the EPR data, a weak π bonding between pairs of P-related sp hybrids may qualitatively explain the tetragonal EPR centre previously correlated with P [17]. However, we note that the experimental estimate for the concentration of the tetragonal EPR centre is substantially smaller than the total P content, which may imply that this EPR centre is not the P donor.

The energy reduction over the on-site defect diminishes with increasing cell size, as do the splittings in the one-electron levels, and we conclude from our calculations that the Jahn–Teller energy for P_s, measured either as the reduction in total energy or by the splitting of the t_2 levels of the on-site defect, is likely to be of the order of tens of meV. The very small energies involved in the distortions suggest that any spectroscopic detection of these centres is likely to be strongly temperature dependent.

Indeed, the isotropic defect detected in P-implanted material [15] might be consistent with a *dynamic* Jahn–Teller effect, in line with the small values of relaxation energies we have obtained. Such a dynamic effect is seen experimentally in the case of the neutral vacancy in diamond [29]. If the small calculated Jahn–Teller energies, and hence a dynamic picture, are correct, then the observation of lower-symmetry centres in experiment would logically correspond to centres perturbed, perhaps by local strains, stabilizing one particular distortion.

We note that in the limit of a weak Jahn–Teller effect, the vibronic band structure should be considered by coupling degenerate vibrational and electronic states. However, such analysis is outside the Born–Oppenheimer approximation, and we have not addressed these issues in this study. If, however, further experimental data indicate that the lower-symmetry centres observed via EPR are not the isolated phosphorus donors, then a full analysis including the vibronic coupling would be essential in understanding this defect.

Acknowledgment

JPG and PRB acknowledge the financial support of the Engineering and Physical Sciences Research Council UK.

References

[1] Farrer R 1969 *Solid State Commun.* **7** 685
[2] Kajihara S A, Antonelli A, Bernholc J and Car R 1991 *Phys. Rev. Lett.* **66** 2010–3
[3] Wang L G and Zunger A 2002 *Phys. Rev.* B **66** 161202
[4] Miyazaki T and Okushi H 2001 *Diamond Relat. Mater.* **10** 449–52

[5] Gheeraert E, Koizumi S, Teraji T, Kanda H and Nesládek M 1999 *Phys. Status Solidi* a **174** 39–51
[6] Gaudin O, Troupis D K, Jackman R B, Nebel C E, Koizumi S and Gheeraert E 2003 *J. Appl. Phys.* **94** 5832–43
[7] Koide Y, Koizumi S, Kanda H, Suzuki M, Yoshida H, Sakuma N, Ono T and Sakai T 2005 *Appl. Phys. Lett.* **86** 232105
[8] Nesladek M 2005 *Semicond. Sci. Technol.* **20** R19–27
[9] Koizumi S, Watanabe K, Hasegawa M and Kanda H 2001 *Science* **292** 1899–901
[10] Suzuki M, Yoshida H, Sakuma N, Ono T, Sakai T and Koizumi S 2004 *Appl. Phys. Lett.* **84** 2349–51
[11] Tajani A, Tavares C, Wade M, Baron C, Gheeraert E, Bustarret E, Koizumi S and Araujo D 2004 *Phys. Status Solidi* a **201** 2462–6
[12] Tavares C, Tajania A, Baron C, Jomard F, Koizumi S, Gheeraert E and Bustarret E 2005 *Diamond Relat. Mater.* **14** 522–5
[13] Samsonenko N D, Tokii V V and Gorban S V 1991 *Sov. Phys.—Solid State* **33** 1409–10
[14] Zvanut M E, Carlos W E, Freitas J A Jr, Jamison K D and Hellmer R P 1994 *Appl. Phys. Lett.* **65** 2287–9
[15] Casanova N, Gheeraert E, Deneuville A, Uzan-Saguy C and Kalish R 2000 *Phys. Status Solidi* a **181** 5–10
[16] Graf T, Brandt M S, Nebel C E, Stutzmann M and Koizumi S 2002 *Phys. Status Solidi* a **193** 434–41
[17] Katagiri M, Isoya J, Koizumi S and Kanda H 2004 *Phys. Status Solidi* a **201** 2451–6
[18] Sque S J, Jones R, Goss J P and Briddon P R 2004 *Phys. Rev. Lett.* **92** 017402
[19] Goss J P, Briddon P R, Sque S J and Jones R 2004 *Diamond Relat. Mater.* **13** 684–90
[20] Jackson K, Pederson M R and Harrison J G 1990 *Phys. Rev.* B **41** 12641–9
[21] Lombardi E B, Mainwood A and Osuch K 2004 *Phys. Rev.* B **70** 205201
[22] Larsson K 2002 *Phys. Status Solidi* a **193** 409–14
[23] Larsson K 2003 *Comput. Mater. Sci.* **27** 23–9
[24] Jones R and Briddon P R 1998 *The Ab Initio Cluster Method and the Dynamics of Defects in Semiconductors* (*Semiconductors and Semimetals* vol 51A) (Boston, MA: Academic) chapter 6
[25] Liberman D A 2000 *Phys. Rev.* B **62** 6851–3
[26] Monkhorst H J and Pack J D 1976 *Phys. Rev.* B **13** 5188–92
[27] Castleton C W M and Mirbt S 2004 *Phys. Rev.* B **70** 195202
[28] Goss J P, Coomer B J, Jones R, Shaw T D, Briddon P R, Rayson M and Öberg S 2001 *Phys. Rev.* B **63** 195208
[29] Davies G 1981 *Rep. Prog. Phys.* **44** 787–830